Journal of Applied Polymer Science

Polyamide/polyacrylonitrile thin film composites as forward osmosis membranes

Parisa Hajighahremanzadeh, Mahsa Abbaszadeh, Seyyed Abbas Mousavi, Mohammad Soltanieh, Hadi Bakhshi

Department of Chemical and Petroleum Engineering, Sharif University of Technology, Tehran 11365-11155, Iran
Correspondence to: S. A. Mousavi (E-mail: musavi@sharif.edu)

ABSTRACT: Thin film composites (TFCs) as forward osmosis (FO) membranes for seawater desalination application were prepared. For this purpose, polyacrylonitrile (PAN) as a moderately hydrophilic polymer was used to fabricate support membranes via nonsolvent-induced phase inversion. A selective thin polyamide (PA) film was then formed on the top of PAN membranes via interfacial polymerization reaction of *m*-phenylenediamine and trimesoyl chloride (TMC). The effects of PAN solution concentration, solvent mixture, and coagulation bath temperature on the morphology, water permeability, and FO performance of the membranes and composites were studied. Support membranes based on low PAN concentrations (7 wt %), NMP as solvent and low coagulation bath temperature (0 °C) demonstrated lower thickness, thinner skin layer, more porosity, and higher water permeability. Meanwhile, decreasing the PAN solution concentration lead to higher water permeance and flux and lower reverse salt flux, structural parameter, and tortuosity for the final TFCs. Composites made in *N*,*N*-dimethylformamide presented lower permeance and flux for water and salt and higher salt rejection, structural parameter, and tortuosity. FO assay of the composites showed lower water permeance values in saline medium comparing to pure water. © 2016 Wiley Periodicals, Inc. J. Appl. Polym. Sci. **2016**, *133*, 44130.

KEYWORDS: composites; films; membranes; polyamides

Received 25 December 2015; accepted 25 June 2016
DOI: 10.1002/app.44130

INTRODUCTION

Nowadays, one of the considerable global challenges is the lack of access to clean and safe drinkable water. Depletion of drinkable water resources has become a major financial and complicated problem for governments.[1,2] Seawater desalination is a solution to overcome this shortage. Reverse osmosis (RO) process is the most economical desalination technique for that purpose.[3,4] However, this method suffers from some drawbacks including (1) high hydraulic pressure as driving force for osmosis resulting in high energy consumption, (2) environmental problems associated with the discharge of concentrated brine, and (3) costs for membrane replacement.[5] Hence, forward osmosis (FO) process has been developed as a promising alternative that can reject a wide range of pollutants and has benefits of low hydraulic pressure and fouling tendency. In this process, the osmotic pressure difference is used to drive water molecules across a semipermeable membrane from a diluted feed solution to a concentrated draw medium, while rejecting most solutes.[6,7] This driving force can be much greater than that for RO process that leads to higher theoretical water flux for FO process.[5,8,9]

FO process like other techniques has its own challenges. The most important concerns are (1) lack of an effective membrane with high water flux and salt rejection and (2) internal concentration polarization (ICP) phenomenon due to the diffusion of solutes to the selective layer through an unstirred support membrane of composite.[5,10,11] More recently, many efforts have been made to prepare effective FO membranes with high water permeance and salt rejection besides low ICP, such as the fabrication of asymmetric membranes.[9,12,13] and thin film composite (TFC) membranes.[14–16] TFCs are constructed of a selective thin polyamide (PA) film on a support membrane. The ideal composite for RO application should have a thin, highly porous and hydrophilic support with low tortuosity.[17,18] ICP phenomenon can be worsened when the support membrane is not fully wetted since the air bubbles can block the water transport.[19] Thus, in this study, polyacrylonitrile (PAN) was chosen to fabricate support membrane due to its moderate hydrophilicity comparing to other materials such as polysulfone (PSf), polyethersulfone (PES), polyethylene (PE), and polypropylene (PP).[20] More recently, Klaysom *et al.*[21] have prepared PA/PAN composites for FO process, which focused on tailoring the parameters of the interfacial polymerization process. Zhang *et al.*,[22] have also fabricated PA/PAN composite membranes with enhanced mechanical properties and water permeance for pressure retarded osmosis (PRO) process.

Table I. The Formulation of Different Solutions Used for Fabricating of Support Membranes

Support membrane	PAN concentration (wt %)	Solvent mixture composition		Coagulation bath temperature (C)
		NMP (%)	DMF (%)	
S1	7	100	0	23
S2	10	100	0	23
S3	13	100	0	23
S4	16	100	0	23
S5	7	75	25	23
S6	7	25	75	23
S7	7	0	100	23
S8	7	100	0	0
S9	7	75	25	0
S10	7	25	75	0
S11	7	0	100	0

In this research, the effective parameters during the preparation PAN membrane via nonsolvent-induced phase inversion were optimized to reach support membranes with low thickness, high porosity, and low tortuosity suitable for the fabrication TFCs with high FO performance. For this purpose, the effects of PAN solution concentration, solvent mixture and coagulation bath temperature on the morphology of support membranes and their water permeability were investigated. Later, a PA film was formed on the top of support membranes through interfacial polymerization reaction to fabricate composites. The structure and FO performance of the prepared TFC for seawater desalination were studied.

EXPERIMENTAL

Materials

Industrial grade polyacrylonitrile (PAN, density = 1.15 g/cm^3, molecular weight = 80–100 kD) was purchased from Esfehan Polyacryl Trading Private Company (Isfahan, Iran). *N*-methyl-2-pyrrolidone (NMP) and *N*,*N*-dimethylformamide (DMF) were supplied by Akkin Company (Turkey). *m*-Phenylenediamine (MPD, >99%) and *n*-hexane (98%) were bought from Merck (Germany). Trimesoyl chloride (TMC, 98.0%) and ethanol (99.8%) were provided by Sigma-Aldrich (Germany). Deionized water (DW) was obtained by a household RO water purifier.

Preparation of PAN Support Membranes

PAN support membranes were prepared via nonsolvent-induced phase inversion procedure. Briefly, PAN was dissolved in solvent (NMP, DMF or their mixtures) at 50 °C. The solution was allowed to be degassed overnight and then cast on a glass plate with a thickness of 120 μm, the cast solution. The cast solution was kept at room temperature for 60 s and then immersed in a coagulant DW bath. After 30 min, the formed support membrane was separated from the glass plate and transferred to another DW bath and preserved at least one night before testing. The formulations of PAN solutions and conditions used to fabricate support membranes are collected in Table I.

Preparation of PA/PAN Composites (TFCs)

PA/PAN composites were prepared through the formation of PA film on the top surface (in contact to with glass plate) of support membranes via interfacial polymerization reaction of MPD and TMC. For this purpose, the top surface of support membranes was initially immersed in aqueous MPD solution (3.5 wt %) for 3 min.[12,13] After removing the water droplets, they were contacted with TMC solution in *n*-hexane (0.2 wt %) for 2 min.[16] To complete the polymerization reaction, samples were then heated in an oven at 60–70 °C for 1, 2, or 3 min. Later, membranes were posttreated through immersion in ethanol/distilled water mixture (1/1, v/v) for 5 min. Finally, the prepared TFCs were rinsed with DW and kept in it until testing. The composites were labeled based on their support membrane. For example, composite TFC1 was prepared based on support membrane S1.

Membrane Characterization

The thickness of wet support membranes was measured by a digital micrometer (Mitutoyo, model 500-196-20, Japan). The reported values are an average of five measurements at different locations for each sample. The porosity of the support membranes was determined via a gravimetric method.[11,15,23] Briefly, the wet samples were taped with tissue paper to remove extra surface water and weighed before (m_1, g) and after (m_2, g) drying in a vacuum oven at 50 °C for 1 day. The porosity (ε, %) was calculated according to eq. (1):

$$\varepsilon = \left[\frac{(m_1 - m_2/d_w)}{(m_1 - m_2/d_w) + (m_2/d_p)}\right] \times 100 \quad (1)$$

where, d_w and d_p are the density of water (0.998 g/cm^3) and PAN (1.15 g/cm^3), respectively. The reported values are an average of three measurements for each membrane.

Surface and cross-section of the support membranes and composites were studied via scanning electron microscopy (SEM, model VEGAII, Tescan, Czech Republic). Samples were dried at room temperature for 24 h and fractured in liquid nitrogen. They were then fixed on aluminum pins using double-sided

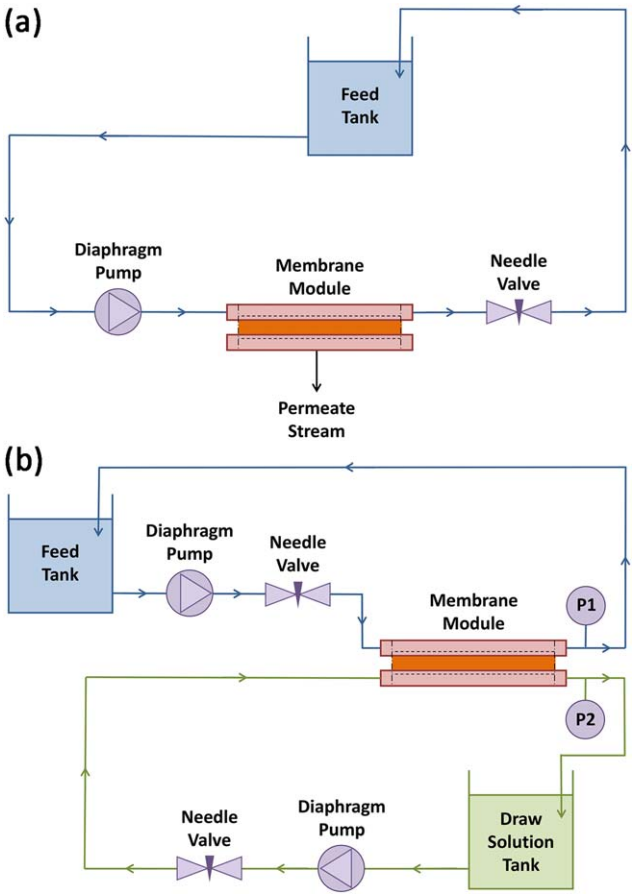

Figure 1. Scheme of laboratory-scale cross flow RO (a) and FO (b) systems used in this study. [Color figure can be viewed in the online issue, which is available at wileyonlinelibrary.com.]

adhesive tape and sputter-coated with a thin gold layer for 4 min. Surface hydrophilicity of the support membranes and composites was determined by measuring the contact angle of water droplets (4 μL) using a contact angle measuring instrument (model OCA 15 plus, Dataphysics Instruments, Germany). Samples were dried in a vacuum oven at 50 °C for 1 day prior to measurements. The reported values are an average of five measurements at different locations for each sample.

RO and FO Experiments

The intrinsic water permeability of support membranes ($A_{w,\mathrm{DW}}$) were measured using a laboratory-scale cross flow RO filtration unit[24] [Figure 1(a)] using DW as feed flowed at room temperature (23 ± 1 °C) and 70 psi pressure. Each run was continued for 2 h and the last half hour data was recorded. The A_w value (L/m^2 h bar) was obtained from the volume of permeated water according to eq. (2)[7,14,20]:

$$A_w = \frac{V_{w,\mathrm{perm}}}{S_m \times t \times \Delta p} \tag{2}$$

where, $V_{w,\mathrm{perm}}$ is the volume of permeated water (L) obtained from its mass and density of water (0.998 g/cm^3), S_m is the effective area of membrane (m^2) in contact with feed, t is the permeation time (0.5 h), and Δp is the difference of hydraulic pressures (bar) between two sides of sample.

This RO filtration unit[24] [Figure 1(a)] was also used to study the RO performance of the composites using NaCl solution (2 g/L) as feed flowed at room temperature (23 ± 1 °C) and 70 psi pressure. The water permeance for TFCs ($A_{w,\mathrm{NaCl}}$) was calculated according to eq. (2)[7,14,20] The salt rejection (R_s) value (%) was obtained using the concentrations of NaCl in the feed ($C_{s,F}$, g/L) and permeate ($C_{s,\mathrm{perm}}$, g/L) solutions, determined via conductivity measurements, according to eq. (3)[7,14,20]:

$$R_s = \left(1 - \frac{C_{s,\mathrm{perm}}}{C_{s,F}}\right) \times 100 \tag{3}$$

The salt permeability (B_s) value (L/m^2 h) was determined using the obtained $A_{w,\mathrm{NaCl}}$ and R_s values and osmotic pressure difference across the sample ($\Delta\pi$) according to eq. (4)[7,11,15]:

$$B_s = \frac{A_w \times (1 - R_s) \times (\Delta p - \Delta\pi)}{R_s} \tag{4}$$

The FO performance of TFCs was studied using a laboratory-scale cross flow FO filtration unit[24] [Figure 1(b)]. The permeation cell contained a rectangular channel on each side of the sample. Due to using a sintered wire mesh laminate in draw solution channel, a spacer was employed to prevent the contact between the surfaces of ragged sintered wire mesh laminate and sample. DW and diluted NaCl medium (3.5 wt %) as feed solution and concentrated NaCl medium (1 and 2 mol/L) as draw solution were used.[24] The flow velocities of both streams were 0.75 L/min, which cocurrently flowed through the channels at room temperature (23 ± 1 °C). The initial volume of both solutions was 2 L. Due to low volume ratio of the permeated water to draw solution (<2%), it was assumed that NaCl concentration of the draw solution and consequently the driving force did not change during FO assay. Water permeation flux (J_w, L/m^2 h) was obtained according to eq. (5):

$$J_w = \frac{V_{w,\mathrm{perm}}}{S_m \times t}. \tag{5}$$

Salt reverse flux (J_s, g/m^2 h) from draw solution to feed medium was obtained according to eq. (6):

$$J_s = \frac{C_{s,f} \times V_f - C_{s,i} \times V_i}{S_m \times t} \tag{6}$$

where, $C_{s,i}$ and $C_{s,f}$ (g/L) are the initial and final NaCl concentrations of the feed solution, respectively, determined by measuring their conductivity, and V_i and V_f (L) are respectively the volumes of feed solution at the beginning and end of the assay.

Structural parameter (S, m) and tortuosity of membrane (τ) of composites were obtained according to eq. (7):

$$S = k \times D_{\mathrm{NaCl}} = \frac{\tau \times l}{\varepsilon} \tag{7}$$

where, D_{NaCl} is diffusion coefficient of NaCl in water that is 1.61 × 10^{-9} m^2/s or 5.80 × 10^{-6} m^2/h at 22.5 ± 1.5 °C,[25] l is the sample thickness (m), ε is the porosity of sample, and K is the solute diffusion resistivity within the sample (m^2 h/L) obtained from eq. (8)[11,15]:

$$K = \frac{1}{J_w} \ln\left(\frac{A\pi_{D,b} + B}{A\pi_{F,m} + B + J_w}\right) \tag{8}$$

where, $\pi_{D,b}$ and $\pi_{F,m}$ are the osmotic pressures (bar) for the bulk of draw solution and feed medium at the composite surface, respectively.

Table II. Thickness, Porosity, and Intrinsic Water Permeability of Support Membranes Obtained From RO Assay Using DW as Feed Solution With a Flow Rate of 0.75 L/min at 70 psi and Room Temperature (23 ± 1 °C)

Support membrane	l at wet stage (μm)	ε (%)	$A_{w,DW}$ (L/m^2 h bar)
S1	84.0 ± 5.4	90.1 ± 0.3	135 ± 7
S2	92.5 ± 7.3	85.0 ± 0.1	108 ± 5
S3	155 ± 6	75.5 ± 0.2	104 ± 5
S4	228 ± 3	69.2 ± 2.9	109 ± 5
S5	69.0 ± 8.2	89.6 ± 0.8	111 ± 6
S6	71.0 ± 9.2	89.9 ± 1.3	98.0 ± 5
S7	65.0 ± 3.3	86.6 ± 2.0	85.9 ± 4
S8	68.0 ± 4.2	87.8 ± 1.4	120 ± 6
S9	60.0 ± 4.7	87.3 ± 0.1	122 ± 6
S10	60.0 ± 2.2	87.1 ± 0.2	96.8 ± 5
S11	54.0 ± 7.6	86.4 ± 0.2	137 ± 7

The sample codes are described in Table I.

RESULTS AND DISCUSSION

Synthesis and Characterization of Support Membranes

An ideal support membrane to manufacture TFC for FO desalination should have a low thickness, high porosity with interconnectional pores, high wettability and low tortuosity.[11,26,27] These features provide a straight way for solutes to pass the support membrane and reach the vicinity of the selective layer in a short time. Low thickness of support membrane not only reduces the potential ICP problem but also facilitates the formation of finger-like macro-voids that span whole this layer. These macro-voids reduce the diffusion resistance of solutes and consequently cause higher water flux.[12] For this purpose, low concentrations of PAN solution, compared to other similar FO membranes,[12,13,22] and low casting thickness were considered in this study to prepare PAN support membrane.

Appropriate hydrophilicity of support membrane can provide sufficient wettability for continuousness distribution of water molecules within the composite and subsequently reduces the ICP phenomenon.[19] The surface hydrophilicity of PAN membranes was evaluated by measuring the water contact angle. The water contact angle value for top surface of S1 was 44 ± 2°, which is lower in comparison with other polymers, e.g., PSf (85°)[16], PES (77°)[11], cellulose acetate (72°)[23], dopamine-coated PSf (54°)[16], and PSf containing 0.5% polyvinylpyrrolidone (55°)[26]. It shows the higher ability of PAN membrane for wetting during FO process.

Effect of PAN Solution Concentration. PAN solutions with different concentrations (7–16 wt %) were cast to prepare support membranes (S1–S4). The thickness and porosity of the prepared support membranes are collected in Table II. Lower PAN concentrations yielded thinner and more porous support membranes, which is favorable for water flux for the final TFCs.

The cross-sectional morphology of the support membranes was studied via SEM (Figure 2). S4 based on 16% PAN concentration showed a dense skin layer on top (in contact with glass plate, max 1 μm) followed with finger-like pores (max 5 μm internal diameter) and then narrow oblique channels (max 30 μm internal diameter) with relatively thick walls (max 10 μm) in bulk. On the other hand, S1 based on 7% PAN concentration demonstrated a thinner dense skin layer (max 0.2 μm), less number of finger-like pores and wider channels with thinner walls. Thus, it can be concluded that using lower PAN concentrations resulted in support membranes with thinner skin layer and more porous structure. In general, higher PAN concentration leads to a more viscous solution and consequently lower coagulation rate (reduced mass transport rate during demixing of solvent and nonsolvent and slower precipitation of polymer chains).[12] Additionally, the polymer precipitation crosses the binodal curve at higher concentrations in polymer/solvent/nonsolvent.[12,28] These phenomena yield a support membrane with thicker skin layer, narrower channels, and thicker walls.[12,29]

Both S1 and S4 showed smooth top surfaces without any voids or pores (Figure 3). This smooth top surface is more favorable for producing a widespread PA film via interfacial polymerization reaction.[13] Meanwhile, the back surface of S1 was more rough and porous than that of S4. In fact, having a lower PAN solution concentration brings out an open back surface with larger pores for support membrane.[28] In contrast, higher PAN solution concentration results in more and smaller nuclei and consequently a dense back surface will be formed.[28] Observing the open back surface for S1 indicated the spread of channels through its whole thickness, which will facilitate the water permeation through it.

To compare the ability of these support membranes to permeate the water molecules, their intrinsic water permeability was measured via a laboratory-scale RO filtration unit using DW as feed. The results are collected in Table II. As expected, S1 with lower PAN solution concentration displayed higher water permeability ($A_{w,DW}$, 135 L/m^2 h bar) due to its lower thickness and higher porosity. Meanwhile, S4 demonstrated partially higher $A_{w,DW}$ value in comparison with S3 in spite of its higher thickness and lower porosity. This can be attributed to its better mechanical property arisen from higher polymer content that reduces the compaction membrane structure during RO assay.

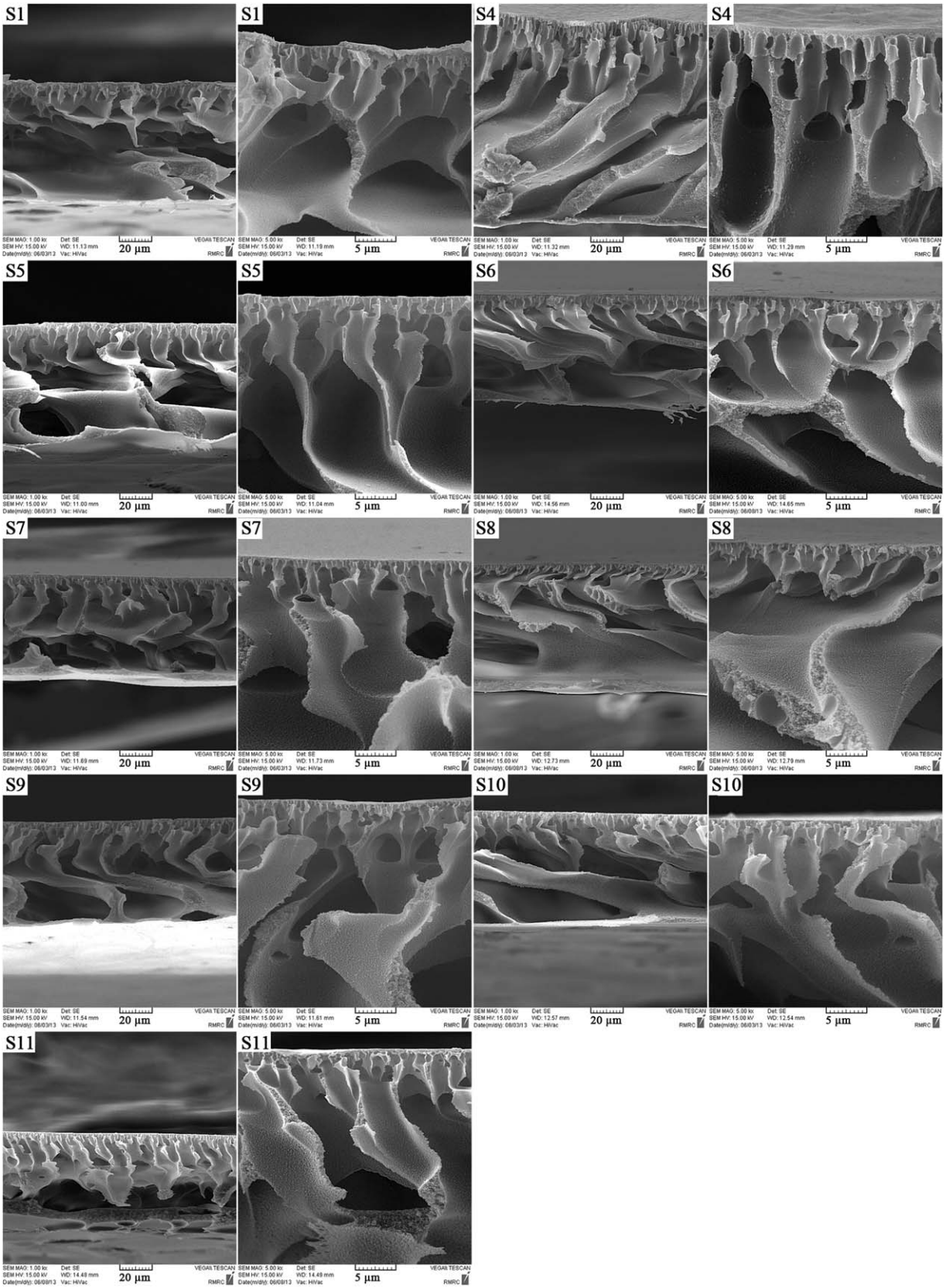

Figure 2. SEM images for a cross-section of support membranes. The sample codes are described in Table I.

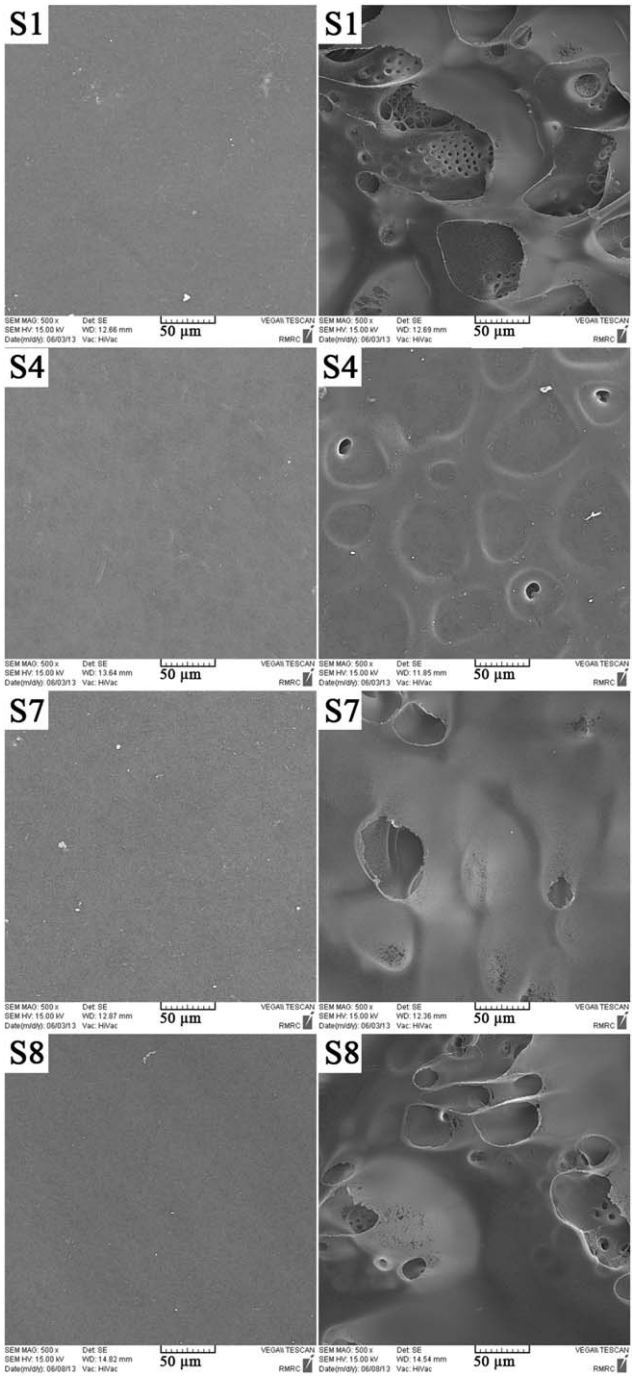

Figure 3. SEM images of the top and back surface of support membranes. The samples codes are described in Table I.

It is worth to mention that this test was repeated for S1 with NaCl solution instead of DW, which resulted in similar water permeability value. This showed, as expected, the PAN support membranes are in ultrafiltration range and cannot desalinate the seawater solely. Lower thickness, more porosity and open back surface for support membrane will cause higher water flux for the final TFCs. Therefore, casting solution with the low PAN concentration (7 wt %) was chosen in continue.

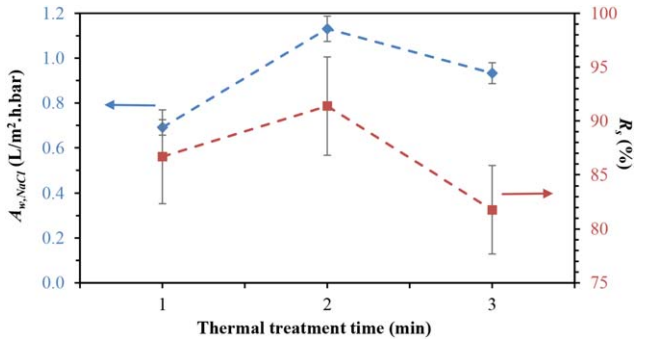

Figure 4. Water permeance and salt rejection for TFC1 treated at 60–70 °C for different times. Values obtained from RO assay using NaCl solution (2 g/L) as feed solution with a flow rate of 0.75 L/min at 70 psi and room temperature (23 ± 1 °C). [Color figure can be viewed in the online issue, which is available at wileyonlinelibrary.com.]

Effect of Solvent Mixture. NMP, DMF, and their mixtures were used as water-miscible solvents to dissolve PAN for the preparation of support membranes. According to Table II, for both coagulant bath temperatures (23 and 0 °C), a slightly reduction in thickness (max 11%) of support membranes were detected by the incorporation of DMF in the solvent mixture. The changes of porosity were also negligible (max 5% reduction), especially at 0 °C.

According to SEM images, for both coagulant bath temperatures, using DMF in solvent mixture did not reform the general morphology of support membranes. Meanwhile, increasing the DMF content in solvent mixture led to partially thicker skin layer, as well as narrower channels with thicker walls in sub layer. This observation is due to the more affinity of PAN for DMF in comparison with NMP, which can be concluded from similar Hildebrand solubility parameter (δ) for PAN (12.4 $cal0^{.5}/cm^{1.5}$) and DMF (12.1 $cal0^{.5}/cm^{1.5}$) comparing to NMP (11.2 $cal0^{.5}/cm^{1.5}$) at 25 °C.[30] Because of this more affinity, the extraction of DMF from PAN solution is more difficult, which keeps out the binodal curve from the polymer-solvent axis in polymer/solvent/nonsolvent ternary-phase diagram, widens the single-phase region and increases the skin layer thickness.[28] Meanwhile, using DMF causes a higher amount of DW needed to precipitate PAN and slower demixing of solvent and nonsolvent, which leads to a denser structure.[31] Due to low PAN concentration and consequently low viscosity of casting solutions,

Table III. Water Permeance, Salt Rejection, and Salt Permeability of TFCs Obtained From RO Assay Using NaCl Solution (2 g/L) as Feed Solution With a Flow Rate of 0.75 L/min at 70 psi and Room Temperature (23 ± 1 °C)

Composite	$A_{w,NaCl}$ (L/m² h bar)	R_s (%)	B_s (L/m² h)
TFC1	1.13 ± 0.06	91.4 ± 4.6	0.335
TFC2	0.750 ± 0.038	97.1 ± 4.9	0.071
TFC3	0.384 ± 0.019	98.5 ± 4.9	0.020
TFC5	1.39 ± 0.07	90.0 ± 4.5	0.485
TFC6	1.26 ± 0.06	95.0 ± 4.8	0.209
TFC7	0.757 ± 0.038	97.9 ± 4.9	0.052

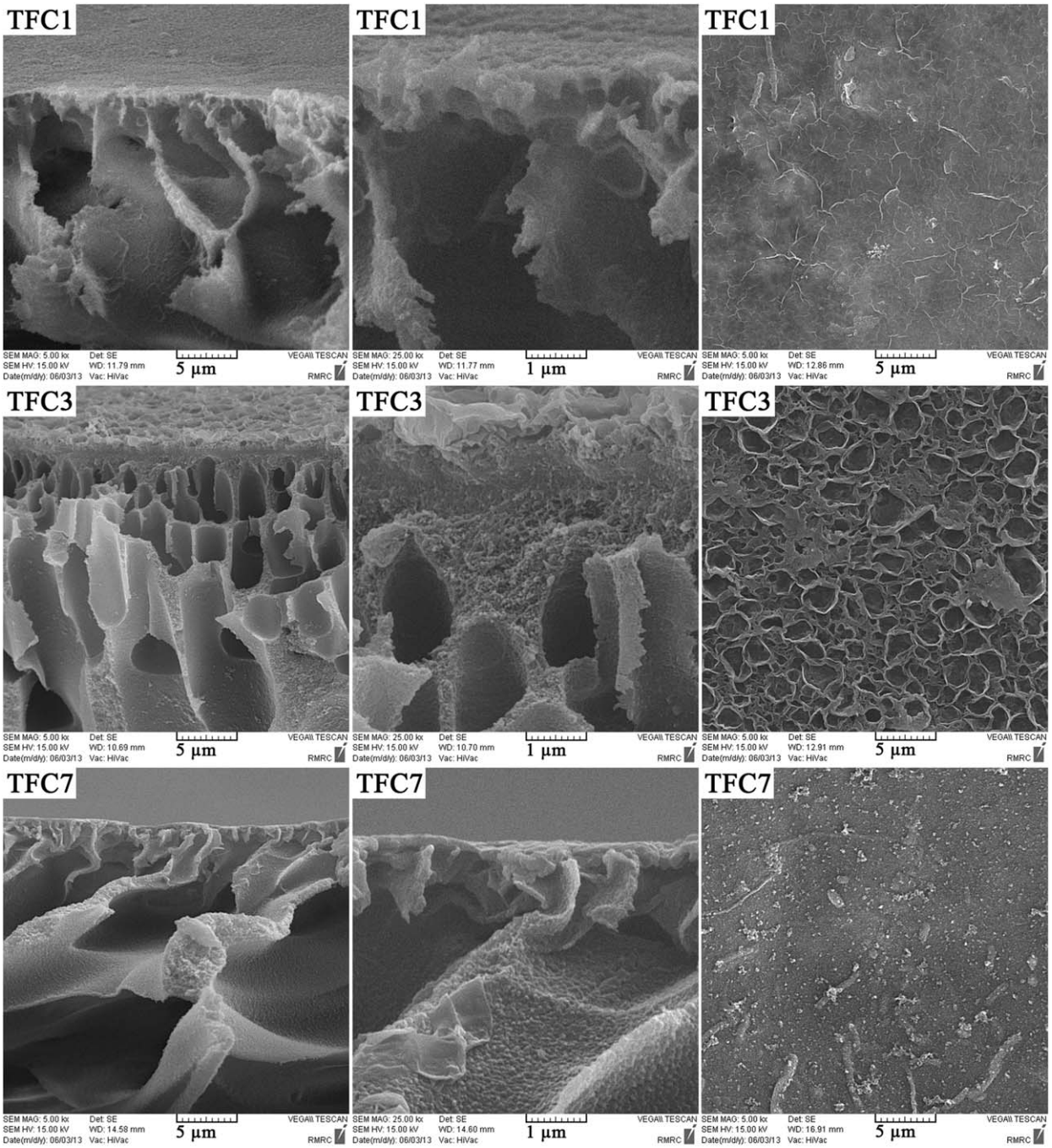

Figure 5. SEM images for cross-section and surface of composites.

we have still faced with finger-like pores formation.[12] The top surface of S7 was as smooth as that of S1 and no evidence of voids or pores was observed. Meanwhile, the back surface of S7 was more even and denser than that of S1. This observation indicated that using DMF as the solvent resulted in a close back surface.

According to Table II, for samples prepared at 23 °C, by increasing the DMF content in the solvent mixture, an obvious decrease in $A_{w,DW}$ value for support membranes was detected. Due to negligible changes of their porosity, this observation can be related to partially thicker skin layer, narrower channels, thicker walls and closer back surface. Reduction of $A_{w,DW}$ value as a result of porosity reduction[32,33] and increase of skin layer thickness[34] has been previously reported.

Effect of Coagulant Bath Temperature. DW with two different temperatures (23 and 0 °C) was used as nonsolvent in coagulant bath. According to Table II, for all solvents, decreasing the temperature of coagulant bath from 23 to 0 °C slightly decreased the thickness (max 15%) and porosity (max 3%) of support membranes. According to SEM images, decreasing

Table IV. Water Flux, Salt Flux, Structural Parameter, Tortuosity, and Porosity Parameter of TFCs Obtained from FO Assay using DW and NaCl Solution (1 mol/L) as Feed and Draw Solutions, Respectively, at Room Temperature (23 ± 1 °C)

Composite	J_w (L/m^2 h)	J_s (g/m^2 h)	S (μm)	τ
TFC1	31.3 ± 1.6	5.11 ± 0.26	112	1.21
TFC2	21.0 ± 1.0	5.07 ± 0.25	165	1.51
TFC3	11.6 ± 0.58	7.05 ± 0.35	260	1.26
TFC5	38.8 ± 1.9	5.34 ± 0.27	88.8	1.15
TFC6	32.5 ± 1.6	4.30 ± 0.22	121	1.83
TFC7	22.8 ± 1.1	3.88 ± 0.19	132	1.76

the bath temperature did not change the general morphology of support membranes, meanwhile, S8 displayed narrower channels with thicker walls comparing to S1. The top surface of S8 was as smooth as that of S1 with no voids or pores, while, the back surface of S8 had slightly less number of voids than S1.

According to Table II, decreasing the temperature from 23 to 0 °C changed the $A_{w,DW}$ value of support membranes, however, this change has no trend. The partial decrease of $A_{w,DW}$ value for S8 comparing to S1 is related to the partial decrease of the internal diameter of channels, thickness of walls and porosity at lower temperature (0 °C).

Synthesis and Characterization of TFCs

TFCs were prepared via the formation of a thin PA layer on top surface of support membranes via interfacial polymerization of MPD and TMC. These reagents are extremely reactive[35] and can make crosslinked (three-dimensional structure) PA film.[34] To complete the interfacial polymerization reaction, the membranes were heated at 60–70 °C. This temperature region was chosen, since the PAN support membranes will collapse at higher temperatures and lose their porosity. Furthermore, thermal treatment at more than 80 °C facilitates the diffusion of monomers within pores of the support membranes before polymerization resulting in a less effective thickness for PA film and thus lower water flux for the final composite.[34,36,37] The optimized time for thermal treatment of TFCs was obtained through heating TFC1 at 60–70 °C in an oven for 1, 2, or 3 min and measuring their water permeance and salt rejection values by RO assay (Figure 4). TFC1 treated for 2 min showed higher $A_{w,NaCl}$ and R_s values. Therefore, all samples were thermally treated for 2 min. The composites were further posttreated via immersion in ethanol/DW mixture (1/1, v/v) for 5 min. Due to a high thickness of S4 (227.5 μm), it was not used for preparing composites.

The surface hydrophilicity of TFCs was also studied by measuring the water contact angle. TFC1 had a contact angle of 66 ± 3°, which showed higher hydrophobicity of PA film in comparison with PAN membrane (44°). The contact angles for aromatic PAs are higher than aliphatic ones. Similar contact angle values were reported for TFCs with a similar composition of PA film by Zhang *et al.* (64.5°)[22] and Ghosh and Hoek (65–70°).[18]

Effect of PAN Solution Concentration. Primarily, the RO performance of the TFCs was studied using NaCl solution (2 g/L) as feed. The results are collected in Table III. TFC1 based on S1 showed higher $A_{w,NaCl}$ value (1.13 L/m^2 h bar) comparing to TFC2 and TFC3. Singh *et al.*,[38] showed that, in the course of interfacial polymerization, the MPD can penetrate inside the pores of support membrane and form PA deep inside the pores yielding a less effective thickness of PA film for water permeation. Higher PAN solution concentration leads to a less porous and more compact skin layer for support layer, which can better prevent the penetration of MPD during PA film formation and thus larger salt rejection and lower salt permeability were recorded for TFC3. This concept is in agreement with the SEM images for cross-section and surface of TFC1 and TFC3 (Figure 5). According to Figure 5, TFC3 displayed a thicker PA layer (1.4 μm) than TFC1 (0.2 μm) with a rougher surface that is typical for a high yield interfacial polymerization on the surface. Huang *et al.*[17] also indicated that the penetration of MPD can change the local MPD/TMC ratio that not only decreases the crosslinking density of the PA layer but increases the PA hydrophilicity due to the generation of some carboxylic acid groups, arisen from unreacted carboxyl chlorides moieties in TMC.[17] They concluded that both of these phenomena facilitate the water permeation through the selective layer.

To study the ability of TFCs for FO desalination, NaCl was used to prepare draw solution due to its low cost, availability, high water solubility, which leads to high osmosis pressure and low fouling.[8,10] Meanwhile, our data will be comparable with other reports. The results are collected in Table IV. FO water fluxes had a trend similar to RO water permeability. TFC1, based on S1 as the most porous support meme bare, showed higher J_w value (31.3 L/m^2 h) comparing to TFC2 and TFC 3 due to its thinner PA film. These observations were similar to previously reported results.[13,39] Salt flux (5.1 g/m^2 h) and structural parameter (112.1 μm) were also lower for TFC1.

Effect of Solvent Mixture. According to Table III, increasing the DMF content in solvent mixture resulted in lower $A_{w,NaCl}$ value for TFC. Higher R_s value and lower B_s values were also detected for composites based on support membrane made

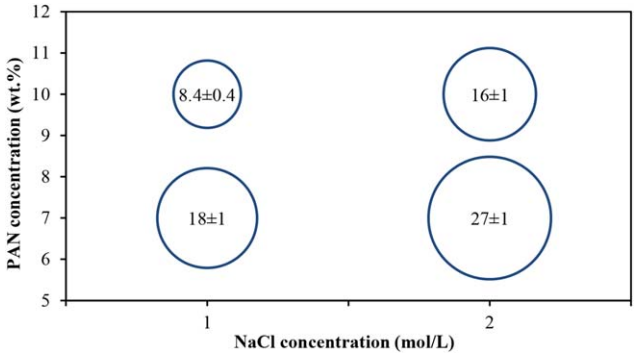

Figure 6. Water flux of TFC1 and TFC2 obtained from FO assay using diluted NaCl medium (3.5 wt %) as feed and concentrated NaCl solutions (1 and 2 mol/L) as draw at room temperature (23 ± 1 °C). [Color figure can be viewed in the online issue, which is available at wileyonlinelibrary.com.]

Table V. A Comparison of FO Performance of Recently Developed Flat Sheet TFCs

Polymers	Feed solution	Draw solution (mol/L)	J_w (L/m^2 h)	S (μm)	References
PA/PSf	DW	NaCl (1)	20.5	389	12
PA/PSf	DW	NaCl (1)	25	312	12
PA/sulfonated PES	DW	NaCl (1)	20	324	41
PA/sulfonated PES	NaCl (3.5 wt %)	NaCl (2)	13.5	324	41
PA/PES nanofiber	DW	NaCl (1)	55	80	27
PA/PES nanofiber	DW	NaCl (1)	47	106	27
PA/modified PSf	NaCl (3.5 wt %)	NaCl (1)	~5	1,510	16
PA/modified PSf	NaCl (3.5 wt %)	NaCl (2)	~7	1,510	16
PA/sulfonated PEK	NaCl (3.5 wt %)	NaCl (2)	~18	107	42
PA/PAN	DW	NaCl (1)	31.3	112.1	This work
PA/PAN	NaCl (3.5 wt %)	NaCl (2)	26.9	164.87	This work

from solvent mixtures with higher DMF content. It is related to partially thicker skin layer for corresponding support membranes, which can prevent the MPD penetration inside their pores[36,37] and thus better formation of PA film. SEM images showed a thickness of 0.2 for PA layer of TFC7 (Figure 5).

According to Table IV, increasing the DMF content in solvent mixture resulted in lower J_w and J_s values for TFCs, which is in agreement with RO results. Meanwhile, using DMF led to higher S and τ for composites. A similar observation has been previously reported for PA/PSf composites.[12] TFC5 with higher J_w value displayed lower S and τ.

Saline FO Performance of Selected TFCs. The ICP phenomenon in FO process is very low or negligible at low NaCl concentrations (<0.4 mol/L).[3,40] Hence, the FO performance of two composites (TFC1 and TFC2) was investigated using diluted NaCl medium (3.5 wt %) as feed and concentrated NaCl solutions (1 and 2 mol/L) as draw. Results are depicted in Figure 6. For both composites, lower J_w values were obtained comparing to that recorded for DW, which is attributed to higher osmosis pressure of feed solution and consequently lower driving force.

In Table V, the FO performance of TFC1 is compared with that of recently reported flat sheet composites. According to Table V, the prepared PAN/PA composites had acceptable FO performance. The low structural parameter value for TFC1 demonstrated the low potential of ICP phenomenon for the prepared TFCs.

CONCLUSIONS

In this study, the effects of PAN solution concentration, solvent mixture and coagulation bath temperature on morphology, RO permeation and FO performance of TFCs were studied. Casting solution with lower PAN concentrations resulted in support membranes with thinner skin layer, more porous and higher $A_{w,DW}$ values. Using DMF in solvent mixture lead to support membranes with partially thicker skin layer and narrower channels with thicker walls in sub layer as well as lower $A_{w,DW}$ values. Decreasing the temperature of coagulant bath from 23 to 0 °C slightly decreased the thickness (max 15%) and porosity (max 3%) of support membranes, while did not change the general morphology of support membranes. Decreasing the PAN solution concentration lead to higher $A_{w,NaCl}$ and J_w, and lower J_s, S, and τ values for the final composites. TFCs based on high DMF content in solvent mixture showed lower $A_{w,NaCl}$, B_s, J_w, and J_s and higher R_s, S, and τ values. Saline FO performance of two composites (TFC1 and TFC2) using diluted NaCl medium (3.5 wt %) and concentrated NaCl solutions (1 or 2 mol/L) as feed and draw solutions showed lower J_w values comparing to that recorded for DW.

NOMENCLATURE

$A_{w,DW}$	intrinsic water permeability obtained from DW flux (L/m^2 h bar)
$A_{w,NaCl}$	water permeance obtained from NaCl solution flux (L/m^2 h bar)
B_s	salt permeability (L/m h)
C_s	salt concentration (mol/L)
D_{NaCl}	diffusion coefficient of NaCl in the membrane substrate (m^2/s)
J_s	reverse salt flux (g/m^2 h)
J_w	water flux (L/m^2 h)
K	solute diffusion resistivity within the porous layer (s/m)
l	thickness (m)
m	membrane weight (g)
ε	porosity (%)
π	osmotic pressure (bar)
p	hydraulic pressure (bar)
R_s	solute rejection (%)
S	membrane structural parameter (m)
S_m	effective membrane surface area (m^2)
t	operation time interval (h)
V	volume of the feed or permeate (L)
ρ	density of the polymer or water (g/cm^3)
τ	tortuosity

SUBSCRIPTS

s	solute
m	membrane
b	bulk solution
D	draw solution side
F	feed solution side

w water
p polymer
Δ() differences between

REFERENCES

1. Shannon, M. A.; Bohn, P. W.; Elimelech, M.; Georgiadis, J. G.; Mariñas, B. J.; Mayes, A. M. *Nature* **2008**, *452*, 301.
2. Montgomery, M. A.; Elimelech, M. *Environ. Sci. Technol.* **2007**, *41*, 17.
3. Zhao, S.; Zou, L.; Tang, C. Y.; Mulcahy, D. *J. Membr. Sci.* **2012**, *396*, 1.
4. Greenlee, L. F.; Lawler, D. F.; Freeman, B. D.; Marrot, B.; Moulin, P. *Water Res.* **2009**, *43*, 2317.
5. Sairam, M.; Sereewatthanawut, E.; Li, K.; Bismarck, A.; Livingston, A. G. *Desalination* **2011**, *273*, 299.
6. Klaysom, C.; Cath, T. Y.; Depuydt, T.; Vankelecom, I. F. J. *Chem. Soc. Rev.* **2013**, *42*, 6959.
7. Cath, T. Y.; Childress, A. E.; Elimelech, M. *J. Membr. Sci.* **2006**, *281*, 70.
8. Zhao, S.; Zou, L. *Desalination* **2011**, *278*, 157.
9. Wang, K. Y.; Ong, R. C.; Chung, T. S. *Ind. Eng. Chem. Res.* **2010**, *49*, 4824.
10. Chung, T. S.; Zhang, S.; Wang, K. Y.; Su, J.; Ling, M. M. *Desalination* **2012**, *287*, 78.
11. Widjojo, N.; Chung, T. S.; Weber, M.; Maletzko, C.; Warzelhan, V. *J. Membr. Sci.* **2011**, *383*, 214.
12. Tiraferri, A.; Yip, N. Y.; Phillip, W. A.; Schiffman, J. D.; Elimelech, M. *J. Membr. Sci.* **2011**, *367*, 340.
13. Yip, N. Y.; Tiraferri, A.; Phillip, W. A.; Schiffman, J. D.; Elimelech, M. *Environ. Sci. Technol.* **2010**, *44*, 3812.
14. Ghosh, A. K.; Bindal, R. C.; Prabhakar, S.; Tewari, P. K. *Desalin. Water Treat.* **2014**, *52*, 432.
15. Wang, K. Y.; Chung, T. S.; Amy, G. *AlChE J.* **2012**, *58*, 770.
16. Han, G.; Zhang, S.; Li, X.; Widjojo, N.; Chung, T. S. *Chem. Eng. Sci.* **2012**, *80*, 219.
17. Huang, L.; McCutcheon, J. R. *J. Membr. Sci.* **2015**, *483*, 25.
18. Ghosh, A. K.; Hoek, E. M. V. *J. Membr. Sci.* **2009**, *336*, 140.
19. McCutcheon, J. R.; Elimelech, M. *J. Membr. Sci.* **2008**, *318*, 458.
20. Jung, B.; Yoon, J. K.; Kim, B.; Rhee, H. W. *J. Membr. Sci.* **2005**, *246*, 67.
21. Klaysom, C.; Hermans, S.; Gahlaut, A.; Van Craenenbroeck, S.; Vankelecom, I. F. J. *J. Membr. Sci.* **2013**, *445*, 25.
22. Zhang, S.; Fu, F.; Chung, T. S. *Chem. Eng. Sci.* **2013**, *87*, 40.
23. Zhang, S.; Wang, K. Y.; Chung, T. S.; Chen, H.; Jean, Y. C.; Amy, G. *J. Membr. Sci.* **2010**, *360*, 522.
24. Cath, T. Y.; Elimelech, M.; McCutcheon, J. R.; McGinnis, R. L.; Achilli, A.; Anastasio, D.; Brady, A. R.; Childress, A. E.; Farr, I. V.; Hancock, N. T. *Desalination* **2013**, *312*, 31.
25. Gray, G. T.; McCutcheon, J. R.; Elimelech, M. *Desalination* **2006**, *197*, 1.
26. Wei, J.; Qiu, C.; Tang, C. Y.; Wang, R.; Fane, A. G. *J. Membr. Sci.* **2011**, *372*, 292.
27. Song, X.; Liu, Z.; Sun, D. D. *Adv. Mater.* **2011**, *23*, 3256.
28. Bokhorst, H.; Altena, F. W.; Smolders, C. A. *Desalination* **1981**, *38*, 349.
29. Smolders, C. A.; Reuvers, A. J.; Boom, R. M.; Wienk, I. M. *J. Membr. Sci.* **1992**, *73*, 259.
30. Hansen, C. M. Hansen Solubility Parameters: A User's Handbook; CRC Press: USA, **2012**.
31. Chun, K. Y.; Jang, S. H.; Kim, H. S.; Kim, Y. W.; Han, H. S.; Joe, Y. *J. Membr. Sci.* **2000**, *169*, 197.
32. Saljoughi, E.; Mohammadi, T. *Desalination* **2009**, *249*, 850.
33. Ferjani, E.; Lajimi, R. H.; Deratani, A.; Roudesli, M. S. *Desalination* **2002**, *146*, 325.
34. Cadotte, J. E. U.S. Pat. 4,277,344 (**1981**).
35. Peng, J.; Su, Y.; Chen, W.; Zhao, X.; Jiang, Z.; Dong, Y.; Zhang, Y.; Liu, J.; Xingzhong, C. *J. Membr. Sci.* **2013**, *427*, 92.
36. Fathizadeh, M.; Aroujalian, A.; Raisi, A. *Desalination* **2012**, *284*, 32.
37. Song, Y.; Liu, F.; Sun, B. *J. Appl. Polym. Sci.* **2005**, *95*, 1251.
38. Singh, P. S.; Joshi, S. V.; Trivedi, J. J.; Devmurari, C. V.; Rao, A. P.; Ghosh, P. K. *J. Membr. Sci.* **2006**, *278*, 19.
39. Qiu, C.; Setiawan, L.; Wang, R.; Tang, C. Y.; Fane, A. G. *Desalination* **2012**, *287*, 266.
40. Zhao, S.; Zou, L. *J. Membr. Sci.* **2011**, *379*, 459.
41. Su, J.; Yang, Q.; Teo, J. F.; Chung, T. S. *J. Membr. Sci.* **2010**, *355*, 36.
42. Han, G.; Chung, T. S.; Toriida, M.; Tamai, S. *J. Membr. Sci.* **2012**, *423*, 543.